Applied Physics Letters

Point defects and dopants of boron arsenide from first-principles calculations: Donor compensation and doping asymmetry

Cite as: Appl. Phys. Lett. **113**, 212101 (2018); https://doi.org/10.1063/1.5062267
Submitted: 24 September 2018 . Accepted: 26 October 2018 . Published Online: 19 November 2018

S. Chae, K. Mengle, J. T. Heron, and E. Kioupakis

View Online

Export Citation

CrossMark

ARTICLES YOU MAY BE INTERESTED IN

Impurity-derived p-type conductivity in cubic boron arsenide
Applied Physics Letters **113**, 251902 (2018); https://doi.org/10.1063/1.5058134

Band structure and carrier effective masses of boron arsenide: Effects of quasiparticle and spin-orbit coupling corrections
Applied Physics Letters **114**, 022101 (2019); https://doi.org/10.1063/1.5062845

Seeded growth of boron arsenide single crystals with high thermal conductivity
Applied Physics Letters **112**, 031903 (2018); https://doi.org/10.1063/1.5004200

Lock-in Amplifiers up to 600 MHz
starting at
$6,210

Zurich Instruments
Watch the Video

AIP Publishing

© 2018 Author(s).

Point defects and dopants of boron arsenide from first-principles calculations: Donor compensation and doping asymmetry

S. Chae, K. Mengle, J. T. Heron, and E. Kioupakis[a)]
Department of Materials Science and Engineering, University of Michigan, Ann Arbor, Michigan 48109, USA

(Received 24 September 2018; accepted 26 October 2018; published online 19 November 2018)

We apply hybrid density functional theory calculations to identify the formation energies and thermodynamic charge transition levels of native point defects, common impurities, and shallow dopants in BAs. We find that As_B antisites, boron-related defects such as V_B, B_{As}, and B_i-V_B complexes, and antisite pairs are the dominant intrinsic defects. Native BAs is expected to exhibit p-type conduction due to the acceptor-type characteristics of V_B and B_{As}. Among the common impurities we explored, we found that C substitutional defects and H interstitials have relatively low formation energies and are likely to contribute free holes. Interstitial hydrogen is surprisingly also found to be stable in the neutral charge state. Be_B, Si_{As}, and Ge_{As} are predicted to be excellent shallow acceptors with low ionization energy ($<$0.03 eV) and negligible compensation by other point defects considered here. On the other hand, donors such as Se_{As}, Te_{As} Si_B, and Ge_B have a relatively large ionization energy ($\sim$0.15 eV) and are likely to be passivated by native defects such as B_{As} and V_B, as well as C_{As}, H_i, and H_B. The hole and electron doping asymmetry originates from the heavy effective mass of the conduction band due to its boron orbital character, as well as from boron-related intrinsic defects that compensate donors. *Published by AIP Publishing.*
https://doi.org/10.1063/1.5062267

Boron arsenide (BAs), a III–V zincblende semiconductor, has received attention recently due to the theoretical prediction[1] and subsequent synthesis and experimental validation[2–4] of its unusually high thermal conductivity. The observed room-temperature thermal conductivity (1300 W m^{-1} K^{-1}) surpasses all other bulk materials except diamond.[2] However, BAs has several potential advantages compared to diamond in terms of cost-effectiveness and compatibility with existing III–V semiconductor technology. Specifically, BAs may be useful as an active electronic component since it has a similar electronic structure to Si but has a wider band gap.[5] Moreover, BAs, as a member of the group III–V arsenide series (BAs-AlAs-GaAs-InAs) or boron series (BP-BAs-BN), can be applicable for alloying conventional III–V semiconductors.[6] Therefore, BAs is a promising material for applications in microelectronics for which efficient heat dissipation is crucial for the performance of devices.

In spite of its attractive thermal properties, the semiconducting properties of BAs have been relatively unexplored. The primary reason is the difficulty in fabricating reasonably large and pure single-crystal samples: though there have been attempts to synthesize BAs crystals over the past 50 years, the high volatility of elemental arsenic, the formation of vacancy defects and grain boundaries, as well as the formation of non-stoichiometric phases degraded the crystal quality.[7–9] However, millimeter-size crystals have recently been synthesized with chemical vapor transport[3] and enable characterization of their fundamental electronic properties.

Besides the intrinsic bulk properties of a semiconductor, native point defects and dopants are important for determining the characteristics of devices. For instance, donor and acceptor incorporation is an essential step in semiconductor technology to achieve the desired type and level of electrical conductivity. In addition, the perturbations of the crystal potential caused by defects decrease the electrical and thermal conductivity. First-principles calculations are a powerful tool to understand the point-defect properties since experimental studies to identify and characterize defects at the atomic scale are challenging. Although the effects of intrinsic defects on the thermal conductivity of BAs have been previously explored,[10,11] there are no reports investigating the role of defects and dopants on its electrical properties.

In this work, we study the thermodynamic properties of point defects in BAs such as native defects, shallow dopants, and common impurity elements, using first-principles calculations. We identified the dominant native and common impurity defects, and we predict that BAs is inherently p-type. Our results show that extrinsic p-type conduction is easier to achieve in BAs than n-type conduction owing to the smaller acceptor ionization energy and negligible acceptor compensation.

We performed first-principles calculations based on hybrid density function theory (DFT) using the projector augmented wave (PAW) method and the Heyd-Scuseria-Ernzerhof (HSE06)[12] functional with 25% mixing as implemented in the Vienna *Ab initio* Simulation Package (VASP).[13–15] The employed PAW pseudopotentials[16,17] include the B $2s^2 2p^1$ and As $4s^2 4p^3$ electrons in the valence with a cutoff energy of 400 eV. All bulk and defect structures were relaxed using the quasi-Newton algorithm with a maximal force criterion of 0.01 eV/Å. Point-defect calculations were performed using a cubic 64-atom supercell with a cell size of 9.54 Å. Spin polarization was considered for supercells with odd numbers of electrons. We performed the supercell size convergence test by comparing to a 216-atom cell and found that the formation energy and transition

a)Author to whom correspondence should be addressed: kioup@umich.edu

energy of a Si atom that substitutes on the B site deviates by less than 0.1 eV after finite-cell-size energy corrections. We used a $2 \times 2 \times 2$ Γ-centered mesh of k-points to sample the first Brillouin zone. However, for the ionization energy of shallow donors and acceptors, the total energies of their neutral and charged states were calculated with a refined $5 \times 5 \times 5$ k-points mesh using the $2 \times 2 \times 2$ k-mesh relaxed atomic structure to include states near the conduction band minimum [approximately near (0.8, 0, 0) in units of $2\pi/a$, where a is the lattice constant]. The formation energy of a point defect D in the charge state of q is determined by[18]

$$E^f(D^q) = E_{tot}(D^q) - E_{tot}(BAs) - \sum n_i(E_i + \mu_i) + q(E_F + E_v) + E_{corr}(D^q), \quad (1)$$

where $E_{tot}(D^q)$ is the total energy of a supercell containing the defect, $E_{tot}(BAs)$ is the total energy of the pristine bulk supercell, n_i is the number of defect atoms added to (or removed from) the supercell, and μ_i and E_i are the chemical potential and energy per i atom in its elemental phase. For charged defects, the formation energy depends on the Fermi level (E_F), which is referenced to the valence-band maximum, E_v. We included an additional correction of 0.07 eV arising from the spin-orbit splitting of the topmost valence bands. The correction energy for the unphysical electrostatic interaction between periodic charged-defects images $E_{corr}(D^q)$ is calculated with the SXDEFECTALIGN code.[19] The static dielectric constant of the host material is $\varepsilon_0 = 9.6$, as determined with density functional perturbation theory[20] and the Quantum ESPRESSO code.[21] The chemical potentials, μ_i, are determined by the growth conditions. The equilibrium condition for the formation of BAs is $\mu_B + \mu_{As} = \Delta H_f(BAs)$, where $\Delta H_f(BAs) = -0.238$ eV is our calculated formation enthalpy of BAs. The chemical potentials for As rich/B poor conditions are bounded by the formation of metallic As [$\mu_{As} = 0$ eV and $\mu_B = \Delta H_f(BAs)$], while As poor/B rich conditions are determined by the formation of elemental B [$\mu_{As} = \Delta H_f(BAs)$ and $\mu_B = 0$ eV]. Other secondary phases we considered for the impurity formation energies are BH_3, h-BN, C_2B_{13}, As_2O_5, AsSi, As_2Ge, As_2Se_3, and As_2Mg_3, while the reference elemental phases are the bulk phases of B, As, C (graphite), Si, Ge, Se, Te, Mg, and Be, and the H_2, O_2, and N_2 molecules. The calculated formation enthalpies of the secondary phases are listed in Table S1.

The calculated properties of bulk BAs are summarized in Table I. Our results show that the HSE hybrid functional with 25% mixing predicts the lattice parameter of BAs in excellent agreement with the experimental values. Although the calculated enthalpy of formation is higher than the experimental value, it affects the defect formation energies by less than 0.17 eV. Our calculated band structure of BAs is shown in Fig. 1(b). The direct and indirect band gaps are found to be 4.13 eV and 1.90 eV, respectively. For comparison, the experimental gap was estimated to be 1.46 eV from photocurrent measurements.[22] However, this result is inconclusive since it was measured from a discontinuous layer of BAs including boron gaps and oxygen contaminants.[22] In comparison with other theoretical results, LDA calculations predict the band gap to be 1.25 eV,[5] and recent GW calculations predict a value of 2.05 eV.[23] Our gap result is therefore in good agreement with the value obtained with the GW method.

TABLE I. Experimental values and HSE06 calculated values for the indirect band gap, lattice parameter, and formation enthalpy of BAs.

	Experimental	Calculated (this work)
a (Å)	4.78[2]	4.77
ΔH_f (eV/f.u.)	−0.408[28]	−0.238
E_g (eV)	1.46[22]	1.90

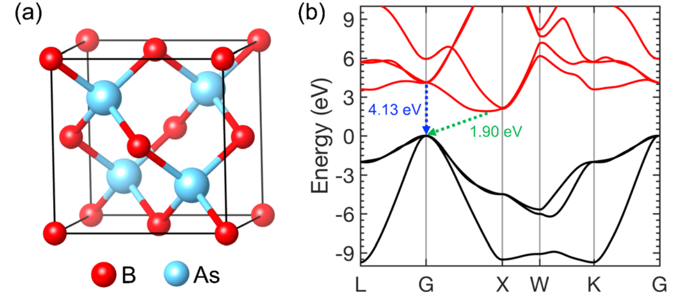

FIG. 1. (a) Zincblende crystal structure of BAs. (b) Calculated band structure of BAs using the HSE hybrid functional. The calculated indirect gap is 1.90 eV and the minimum direct gap at Γ is 4.13 eV.

We first examine intrinsic defects since they are unavoidable during growth and can dramatically affect the electrical and thermal properties. Intrinsic defects we considered include B vacancies (V_B), As vacancies (V_{As}), Schottky defects (V_B-V_{As}), B antisites (B_{As}), As antisites (As_B), antisite pairs (B_{As}-As_B), B interstitials (B_i), As interstitials (As_i), B Frenkel defects (V_B-B_i), and As Frenkel defects (V_{As}-As_i). Their atomic structures are shown in Fig. S1 and their formation energies are plotted as a function of the Fermi energy in Fig. 2 for both As-rich and B-rich conditions. Under both growth conditions, boron-related defects such as B_{As}, V_B, and B_{As}-As_B are predicted to dominate in BAs owing to their lower relative formation energies. B_{As} is a shallow acceptor with an ionization energy of 0.05 eV. It has the lowest formation energy for Fermi energies near CBM, indicating that it is an important donor-passivating defect. However, for Fermi energies near the VBM, B_{As} more likely forms a pair with As_B in the neutral charge state. V_B is also an important native defect in BAs with a relatively low formation energy

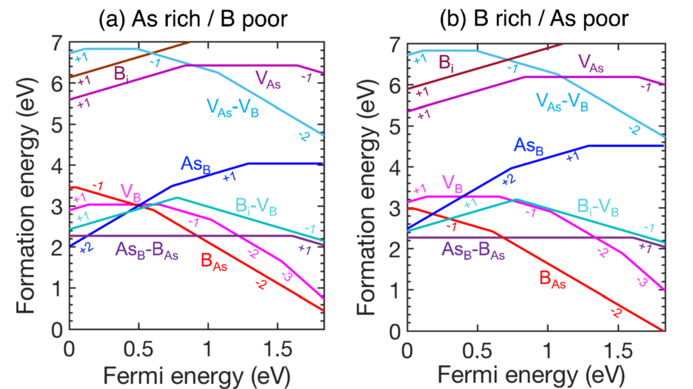

FIG. 2. Formation energy of various intrinsic point defects as a function of the Fermi level in the limit of (a) As-rich/B-poor and (b) B-rich/As-poor growth conditions.

for Fermi energies near the CBM. It is stable in various charge states depending on the Fermi level, but it is a deep acceptor with the 0/−1 transition level at $E_F = 0.66$ eV. On the other hand, As_B is a deep donor defect and is one of the lowest formation energy defects for Fermi energies very near the VBM. However, As_B has a high formation energy compared to the B_{As}-As_B pair for most Fermi energies higher than the VBM, indicating that it is more likely to be stabilized within antisite defect pairs. The concentrations of other defects (interstitials, As vacancies, and Schottky defects) are expected to be negligible under any conditions because of their high formation energy.

We next investigate the common impurity defects related to H, O, N, and C atoms, since these elements are common in the environment in the form of water, atmospheric air, or organic contaminants and are often inadvertently incorporated into a material during growth and post-processing. Our results for their formation energies at the two extreme growth conditions are shown in Fig. 3 and their atomic structures in Fig. S2, while their lowest formation energy over the entire range of chemical potentials is plotted in Fig. S3. Among the various types of impurity defects, we predict that substitutional C defects, both C_{As} and C_B, form easily, possibly owing to the valence of C being the average of B and As. We find that C_B acts like a deep donor with an ionization energy of 0.47 eV, whereas C_{As} is a shallow acceptor with an ionization energy of 0.09 eV. However, in intrinsic BAs, C prefers to occupy the As site rather than the B site and pins the Fermi level from 0.15 eV to 0.40 eV above the VBM depending on the growth conditions. H_i and H_B are also likely to form in BAs due to the small size of H. H_i has a relatively low formation energy throughout the entire Fermi-level range and its charge state varies from +1 to −1. In most semiconductors and insulators, H_i acts as a "negative-U" center that is only stable in the +1 and −1 charge states, and its charge-transition level serves as a universal band-alignment criterion.[24] We surprisingly find that the neutral charge state is also stable in BAs. This unusual result, also observed for interstitial hydrogen in diamond and boron nitride,[25] may be attributed to the small lattice constant of BAs compared to other III–V semiconductors. In addition to C_{As} and H_i, H_B in the −2 charge state has a low formation energy for Fermi energies near the CBM, showing that it is another important charge-compensating defect in n-doped BAs. The concentrations of other defects associated with these four common impurities, such as H_{As}, C_i as well as O- and N-related defects, are negligibly small because of their high formation energies.

We subsequently investigate the possibility of n-type doping of BAs with Se, Te, Si, and Ge dopants. Se and Te are group-16 elements with ionic radii close to that of As^{+5}, and are thus expected to preferentially occupy the As site. On the other hand, since the ionic radii of the group-14 elements (Si and Ge) are comparable to both B^{+3} and As^{+5}, we investigated Si and Ge atoms that substitute both the B-site as donors and the As-site as acceptors for comparison. Our results (Figs. 4 and S4) show that the donor ionization energy (i.e., the 0 to +1 charge transition level) is 0.16 eV for Se_{As}, 0.13 eV for Te_{As}, 0.14 eV for Si_B, and 0.17 eV for Ge_B. We therefore predict that, regardless of the type of donor atom, shallow donors have relatively large ionization energies in BAs. This is in contrast to Si and GaAs, both of which have much smaller donor ionization energies (∼0.05 eV for As, P and Sb donors in Si[26], and ∼0.006 eV for Se, Si, and Ge donors in GaAs[27]) We attribute the large ionization energy of BAs to its heavy electron effective mass that, according to the Bohr model of donor ionization, leads to a large ionization energy and poor donor activation. We also note that although Se and Te preferentially substitute the As site, donating electrons, Si and Ge are more likely to occupy the As site as acceptors rather than serving as donors on the B site. Thus, we conclude that Si and Ge dopants preferentially act as acceptors in BAs. Overall, however, the formation energies of donors are higher than the formation energies of compensating negatively charged intrinsic defects such as B_{As} and V_B, as well as negatively charged C_{As}, H_i, and H_B. Therefore, donors are highly likely to be passivated by boron-related intrinsic defects and potential unintentional impurities in BAs.

We also investigated p-doping of BAs by Be and Mg acceptors on the B-site, as well as Si and Ge acceptors on the As-site. Although we found that Mg_B is energetically unfavorable due to the large ionic-size difference between Mg and B, we predict that Be_B, Si_{As}, and Ge_{As} are excellent shallow acceptors with low ionization energy (<0.03 eV) and sufficiently low formation energy (Fig. 4 and Table II). Their

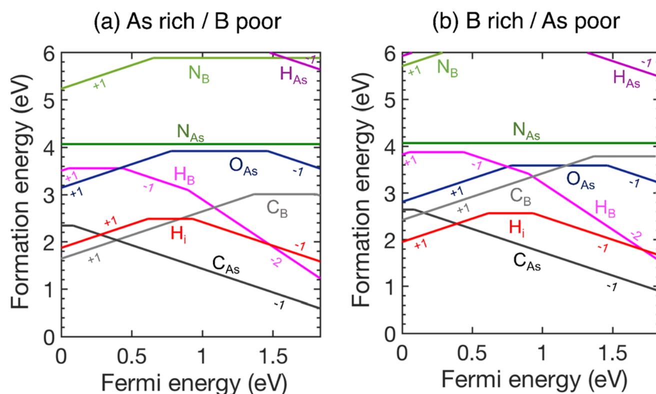

FIG. 3. Formation energy of common impurity defects as a function of the Fermi level in the limit of (a) As-rich/B-poor and (b) B-rich/As-poor growth conditions.

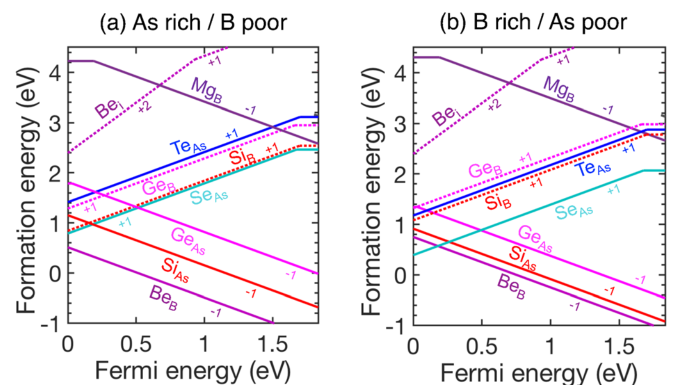

FIG. 4. Formation energy of donor and acceptor impurities as a function of the Fermi level in the limit of (a) As-rich/B-poor and (b) B-rich/As-poor growth conditions.

TABLE II. Shallow donor and acceptor ionization energies of BAs.

Donor	Ionization energy (eV)	Acceptor	Ionization energy (eV)
Se_{As}	0.16	Be_B	<0.03
Te_{As}	0.13	Si_{As}	<0.03
Si_B	0.14	Ge_{As}	0.03
Ge_B	0.17	Mg_B	0.19

maximum formation energies occur at $E_F = VBM$, which are 0.51 eV for Be_B, 0.91 eV for Si_{As}, and 1.35 eV for Ge_{As} under chemical-potential conditions that minimize their formation energy (Fig. S5). Considering the higher formation energies of passivating donor-type intrinsic defects and common impurities (such as As_B, C_B, and H_i) in this Fermi-energy region, shallow acceptors are not likely to be compensated in BAs. We also explored any possible self-compensation from the dopant element themselves when incorporated into undesired sites. Figure S6 shows the formation energies of acceptor species incorporated into interstitial sites of BAs. Interstitial dopants act as donors but they have much higher formation energies compared to substitutional defects, and thus do not incorporate in appreciable concentrations. In addition, Fermi pinning owing to Si or Ge dopants incorporated onto both the B and As sites occurs only for a specific range of chemical potentials. Under As-rich conditions, the formation energies of Si_B and Ge_B in the +1 charge state are slightly lower than Si_{As} and Ge_{As} for Fermi energies near the VBM, thus Be is the best acceptor candidate under these conditions. On the other hand, in As-poor conditions, Si and Ge are stable in the −1 charge state on the As site for the entire range of Fermi energies. Therefore, Be, Si, and Ge can all p-type dope BAs without charge compensation.

In conclusion, we investigated the thermodynamic properties of common defects, impurities, and dopants in BAs with first-principles calculations. Our results show that the unique physical properties of boron result in the doping asymmetry of BAs. The large electron effective mass of BAs that originates from the small radius of the B orbitals leads to relatively large ionization energies of shallow donors. Moreover, donor atoms have higher formation energy than acceptors and are compensated by negatively charged boron-related intrinsic defects and common impurities in BAs such as B_{As}, V_B, C_{As}, H_i, and H_B. On the other hand, excellent p-type dopability of BAs is predicted using Be, Si, and Ge elements with ionization energies less than 0.03 eV. Therefore, our results uncover the fundamental challenges and opportunities of doping BAs for applications in semiconductor devices.

See supplementary material for the formation enthalpies of impurity phases, the atomic structure of defects, the lowest formation energy of common impurities, extrinsic dopants, and interstitial dopants.

We would like to thank Dr. Bing Lv for useful discussions. This work was supported by the Designing Materials to Revolutionize and Engineer our Future (DMREF) Program under Award No. 1534221, funded by the National Science Foundation. K.A.M. acknowledges the support from the National Science Foundation Graduate Research Fellowship Program through Grant No. DGE 1256260. This research used resources of the National Energy Research Scientific Computing Center, a DOE Office of Science User Facility supported by the Office of Science of the U.S. Department of Energy under Contract No. DE-AC02-05CH11231.

[1]L. Lindsay, D. A. Broido, and T. L. Reinecke, Phys. Rev. Lett. **111**, 025901 (2013).
[2]J. S. Kang, M. Li, H. Wu, H. Nguyen, and Y. Hu, Science **361**, 575 (2018).
[3]F. Tian, B. Song, X. Chen, N. K. Ravichandran, Y. Lv, K. Chen, S. Sullivan, J. Kim, Y. Zhou, T. H. Liu, M. Goni, Z. Ding, J. Sun, G. A. G. U. Gamage, H. Sun, H. Ziyaee, S. Huyan, L. Deng, J. Zhou, A. J. Schmidt, S. Chen, C. W. Chu, P. Y. Huang, D. Broido, L. Shi, G. Chen, and Z. Ren, Science **361**, 582 (2018).
[4]S. Li, Q. Zheng, Y. Lv, X. Liu, X. Wang, P. Y. Huang, D. G. Cahill, and B. Lv, Science **361**, 579 (2018).
[5]R. M. Wentzcovitch and M. L. Cohen, J. Phys. C Solid State Phys. **19**, 6791 (1986).
[6]G. L. W. Hart and A. Zunger, Phys. Rev. B **62**, 13522 (2000).
[7]F. V. Williams and R. A. Ruehrwein, J. Am. Chem. Soc. **82**, 1330 (1960).
[8]J. Osugi, K. Shimizu, and Y. Tanaka, Proc. Jpn. Acad. **42**, 48 (1966).
[9]J. A. Perri, S. Laplaca, and B. Post, Acta Crystallogr. **11**, 310 (1958).
[10]Q. Zheng, C. A. Polanco, M. Du, R. Lucas, M. Chi, J. Yan, and B. C. Sales, Phys. Rev. Lett. **121**, 105901 (2018).
[11]N. H. Protik, J. Carrete, N. A. Katcho, N. Mingo, and D. Broido, Phys. Rev. B **94**, 045207 (2016).
[12]J. Heyd, G. E. Scuseria, and M. Ernzerhof, J. Chem. Phys. **118**, 8207 (2003).
[13]G. Kresse and J. Hafner, Phys. Rev. B **47**, 558 (1993).
[14]G. Kresse and J. Furthmüller, Comput. Mater. Sci. **6**, 15 (1996).
[15]G. Kresse and J. Furthmüller, Phys. Rev. B **54**, 11169 (1996).
[16]P. E. Blöchl, Phys. Rev. B **50**, 17953 (1994).
[17]G. Kresse and D. Joubert, Phys. Rev. B **59**, 1758 (1999).
[18]C. Freysoldt, B. Grabowski, T. Hickel, J. Neugebauer, G. Kresse, A. Janotti, and C. G. Van De Walle, Rev. Mod. Phys. **86**, 253 (2014).
[19]C. Freysoldt, J. Neugebauer, and C. G. Van De Walle, Phys. Rev. Lett. **102**, 016402 (2009).
[20]S. Baroni, S. De Gironcoli, A. Dal Corso, S. Scuola, I. Superiore, I. Istituto, F. Materia, I. Trieste, and P. Giannozzi, Rev. Mod. Phys. **73**, 515 (2001).
[21]P. Giannozzi, S. Baroni, N. Bonini, M. Calandra, R. Car, C. Cavazzoni, D. Ceresoli, G. L. Chiarotti, M. Cococcioni, I. Dabo, A. Dal Corso, S. De Gironcoli, U. Gerstmann, C. Gougoussis, A. Kokalj, M. Lazzeri, L. Martin-samos, N. Marzari, F. Mauri, R. Mazzarello, S. Paolini, A. Pasquarello, L. Paulatto, and C. Sbraccia, J. Phys. Condens. Matter **21**, 395502 (2009).
[22]S. Wang, S. F. Swingle, H. Ye, F. R. F. Fan, A. H. Cowley, and A. J. Bard, J. Am. Chem. Soc. **134**, 11056 (2012).
[23]K. Bushick, K. Mengle, N. Sanders, and E. Kioupakis, "Band structure and carrier effective masses of boron arsenide: Effects of quasiparticle and spin-orbit coupling corrections," pre-print arXiv:1809.09549 (2018).
[24]C. G. Van der Walle and J. Neugebauer, Nature **423**, 626 (2003).
[25]J. L. Lyons and C. G. Van De Walle, J. Phys. Condens. Matter **28**, 06LT01 (2016).
[26]W. Kohn, Solid State Phys. **5**, 257 (1957).
[27]A. G. Milnes, *Deep Impurities in Semiconductors* (Wiley, New York, NY, 1973).
[28]H. Dumont and Y. Monteil, J. Cryst. Growth **290**, 410 (2006).